RESEARCH ARTICLE

The dynamic side of the Warburg effect: glycolytic intermediates as buffer for fluctuating glucose and O_2 supply in tumor cells [version 1; referees: 1 approved, 1 approved with reservations]

Johannes H.G.M. van Beek [1,2]

[1]Experimental Vascular Medicine, Amsterdam University Medical Centers, location AMC, Amsterdam, 1105 AZ, Netherlands
[2]Clinical Genetics, Amsterdam University Medical Centers, location VUmc, Amsterdam, 1081 BT, Netherlands

v1 **First published:** 02 Aug 2018, **7**:1177 (doi: 10.12688/f1000research.15635.1)
Latest published: 02 Aug 2018, **7**:1177 (doi: 10.12688/f1000research.15635.1)

Abstract

Background: Tumor cells show the Warburg effect: high glucose uptake and lactate production despite sufficient oxygen supply. Otto Warburg found this effect in tissue slices and in suspensions of Ehrlich ascites tumor cells. Remarkably, these ascites tumor cells can transiently take up glucose an order of magnitude faster than the steady high rate measured by Warburg for hours.
Methods: The purpose of the transiently very high glucose uptake is investigated here with a computational model of glycolysis, oxidative phosphorylation and ATP consumption which reproduces short kinetic experiments on the ascites tumor cells as well as the long-lasting Warburg, Crabtree and Pasteur effects. The model, extended with equations for glucose and O_2 transport in tissue, is subsequently used to predict metabolism in tumor cells during fluctuations of tissue blood flow resulting in cycling hypoxia.
Results: The model analysis suggests that the head section of the glycolytic chain in the tumor cells is partially inhibited in about a minute when substantial amounts of glucose have been taken up intracellularly; this head section of the glycolytic chain is subsequently disinhibited slowly when concentrations of glycolytic intermediates are low. Based on these dynamic characteristics, simulations of tissue with fluctuating O_2 and glucose supply predict that tumor cells greedily take up glucose when this periodically becomes available, leaving very little for other cells. The glucose is stored as fructose 1,6-bisphosphate and other glycolytic intermediates, which are used for ATP production during O_2 and glucose shortages.
Conclusions: The head section of glycolysis which phosphorylates glucose may be dynamically regulated and takes up glucose at rates exceeding the Warburg effect if glucose levels have been low for some time. The hypothesis is put forward here that dynamic regulation of the powerful glycolytic enzyme system in tumors is used to buffer oxygen and nutrient fluctuations in tissue.

Keywords

glycolysis, cancer, hypoxia, cycling hypoxia, nutrient shortage, computational model, cancer metabolism, oxidative phosphorylation, nutrient fluctuation

Open Peer Review

Referee Status: ✔ ?

	Invited Referees 1	2
version 1 published 02 Aug 2018	✔ report	? report

1 **Ranjan K. Dash**, Medical College of Wisconsin and Marquette University, USA

2 **Ziwei Dai**, Duke University School of Medicine, USA

Discuss this article

Comments (0)

Corresponding author: Johannes H.G.M. van Beek (j.h.vanbeek@amc.uva.nl)

Author roles: van Beek JHGM: Conceptualization, Data Curation, Formal Analysis, Investigation, Methodology, Project Administration, Software, Supervision, Validation, Visualization, Writing – Original Draft Preparation, Writing – Review & Editing

Competing interests: No competing interests were disclosed.

Grant information: The author(s) declared that no grants were involved in supporting this work.

How to cite this article: van Beek JHGM. **The dynamic side of the Warburg effect: glycolytic intermediates as buffer for fluctuating glucose and O_2 supply in tumor cells [version 1; referees: 1 approved, 1 approved with reservations]** *F1000Research* 2018, **7**:1177 (doi: 10.12688/f1000research.15635.1)

First published: 02 Aug 2018, **7**:1177 (doi: 10.12688/f1000research.15635.1)

Introduction

Cancer cells often show high lactate production despite sufficient oxygen supply, a phenomenon discovered by Otto Warburg[1], and an example of widespread metabolic reprogramming in cancer[2–4]. Warburg's favorite experimental system to study this effect were suspensions of mouse Ehrlich ascites tumor cells (EATC)[1,5,6], which showed high aerobic glycolytic rates persisting for hours, at least when glucose concentrations remained high. These EATC were later also used by Warburg's contemporaries to study the kinetics of metabolic responses in the first seconds and minutes after glucose addition to cells previously depleted of glucose[7,8], showing that glucose uptake is much higher in the first minute than averaged over one hour. The results of these experiments were explained by Chance and Hess with a mathematical model, which may have been the first digital computer model of a metabolic system[7,9]. Their model contained some biochemical assumptions that are now considered untenable. In the present study, a small computational model is developed that economically reproduces the experimental results of the kinetic as well as the steady-state experiments on Ehrlich ascites tumor cells, and furthermore provides a testable model of the dynamic regulation of energy metabolism in the ascites tumor cells. Analysis of the model suggests that the head section of glycolysis can sequester glucose at very high capacity, but is downregulated quickly to steady-state Warburg effect levels if glucose has been taken up. However, the glycolytic head section is disinhibited slowly if glycolytic intermediates are depleted in the cells.

Because the metabolic model reproduces the behavior of the ascites tumor cells well for conditions with variable glucose levels, it is subsequently used to investigate the possible physiological role of this dynamic metabolic regulation in the tumor cells. Blood flow and the supply of oxygen and nutrients is often fluctuating in tumor tissue, a phenomenon referred to as cycling hypoxia[10–12]. To investigate the role of the dynamic regulation of metabolism, the computational model is extended with equations for oxygen and glucose transport in tumor tissue with cycling blood flow. The simulations reported here suggest that tumor cells can store glucose-derived metabolites to maintain ATP and carbon substrate levels during periodic oxygen and glucose shortages, as are commonly found in tumor tissue[11,13]. As a result, cells with lower glycolytic capacity than tumor cells have sufficient energy supply at constant blood flow, but their energy supply fails in conditions with fluctuating blood flow where tumor cells with high glycolytic capacity still do well.

Methods

Development of the computational model

The simplified computational model developed and applied in this study comprises glycolysis, oxidative phosphorylation, ATP consumption and their interactions in the tumor cell (Figure 1). The goal of the model is to reconstruct the glucose uptake behavior and the dynamic balance of ATP, phosphorylated metabolites, glucose-derived metabolites and NADH/NAD redox status in the cell, especially in the first minute after a challenge. In addition, it also reproduces three effects which persist on the

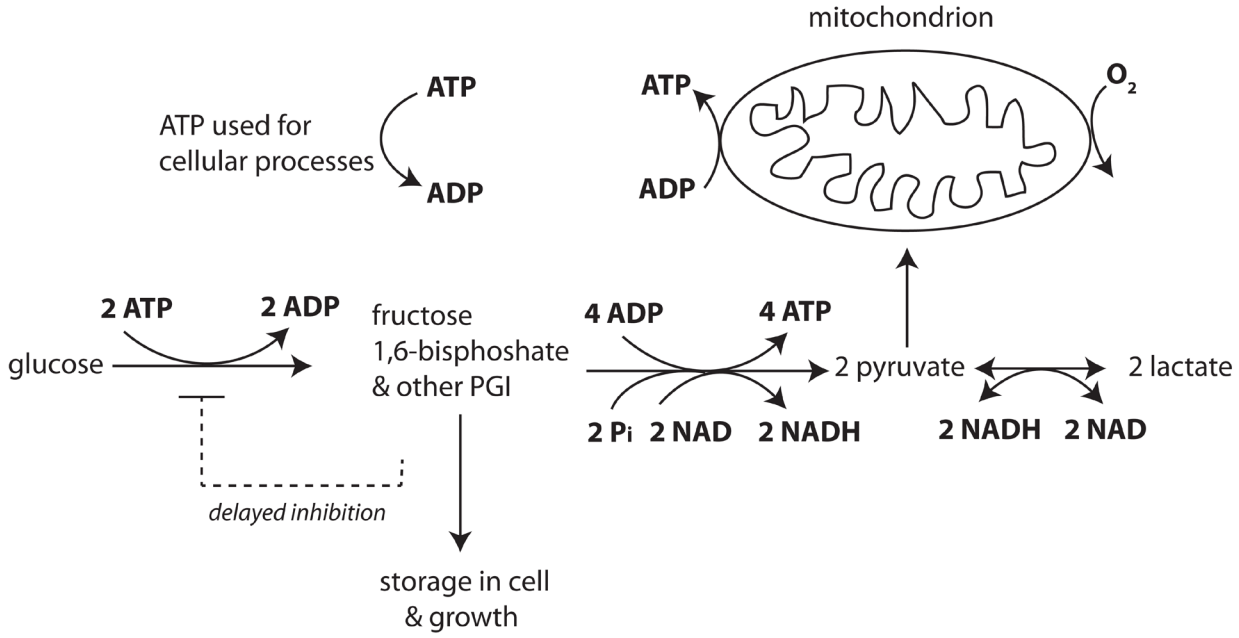

Figure 1. Scheme of computational model of tumor cell metabolism. In the head section of glycolysis, 2 ATP are spent to phosphorylate glucose, resulting in phosphorylated glycolytic intermediates (PGI) with fructose 1,6-bisphosphate (FBP) as major species. In the tail section of glycolysis four ATP, two reduced nicotinamide adenine dinucleotide (NADH) and two pyruvate molecules are produced per metabolized FBP and two inorganic phosphate (P_i) molecules are taken up. Pyruvate molecules can be converted to lactate while producing oxidized NAD. Pyruvate and NADH are also substrates for mitochondrial oxidative metabolism. ATP is used for growth, proliferation and maintenance tasks such as ion pumping. Increased NADH concentration reduces flux in the tail section. Signals from the PGI pool inhibit the head section with a time delay.

order of an hour or longer: i) the Warburg effect[1,6]: high glycolytic rate despite abundant oxygen availability; ii) the Pasteur effect[7]: increase in glycolytic rate when oxygen is depleted; and iii) the Crabtree effect[6,14]: decrease in oxygen uptake after addition of glucose. The computational model consists of rate equations for the head and tail part of glycolysis, oxidative phosphorylation and lactate dehydrogenase which together determine the rate of change of the key metabolites in the model, captured in a system of ordinary differential equations. The model is not meant to be a detailed reconstruction of the enzyme reactions involved and their regulatory mechanisms, but focuses on reproduction of the metabolic responses of the cell which are measured experimentally. Nevertheless, this small model reproduces the three steady effects and a range of kinetic data with satisfactory quantitative approximation.

Chance and Hess[7,9] already had developed a digital computer model to explain measurements of transients in glucose metabolism and mitochondrial respiration in Ehrlich ascites tumor cells. This was probably the first digital model of a biochemical system ever published. However, the model's assumptions are not compatible with present biochemical knowledge: oxidative phosphorylation, for instance, was assumed to occur via a phosphorylated high energy intermediate and not via a chemiosmotic mechanism, and mitochondria were assumed to retain synthesized ATP until an uncoupling agent was applied. Therefore a new model was developed here.

Although glycolysis has been extensively studied, it is presently still difficult to construct a fully detailed accurate model of this pathway[15]. Therefore, a simplified representation of glycolysis by a head and tail section is used, similar to that in old conceptual models[16]. This approach is also taken in recent computational[17,18] models for yeast glycolysis to investigate robustness, efficiency, oscillations, and failure to start up. Consequently, the new model incorporates a parsimonious description capturing the essential kinetic properties of the glycolytic system in mammalian cells. Two kinetic equations represent the head and tail sections of glycolysis upstream and downstream of fructose 1,6-bisphosphate (FBP). These two equations make it possible to calculate the time course of the FBP pool, which can be directly compared with measurements in the experimental data sets. FBP usually also is the most abundant species of the phosphorylated glycolytic intermediates (PGI). The new model presented here further incorporates a simple description of oxidative phosphorylation in the mitochondria, which responds to ADP, inorganic phosphate (P_i) and oxygen concentrations. This equation is compatible with biochemical knowledge and has been used to investigate the functional significance of the creatine kinase energy buffer system in muscle[19]. The equations are discussed in detail in the Supplementary Material. The state variables of the model are given in Supplementary Table 1 and the metabolic fluxes in Supplementary Table 2.

The head section of glycolysis comprises the hexokinase, glucose 6-phosphate isomerase and phosphofructokinase enzymes, which catalyze the double phosphorylation of hexose. The most abundant phosphorylated glycolytic intermediate is FBP, which is directly represented in the model. However, the other phosphorylated glycolytic intermediates (PGI), consisting of glucose 6-phosphate, fructose 6-phosphate, dihydroxyacetone phosphate, 3-phosphoglycerate, etc., are taken into account in the storage of glucose-derived metabolites. They are lumped with FBP in the total PGI pool with a model parameter representing the fixed ratio between the sum of all phosphorylated glycolytic intermediates and FBP. In this way the total PGI content is taken into account in the time-dependent mass balance calculations. The rate of the glycolytic head section depends on glucose and ATP concentrations. The interaction of glucose and ATP in determining the rate of the head section is modelled similarly as in kinetic equations for mammalian hexokinase[20,21], a major site of glycolytic rate limitation in cancer cells[22].

In tumor cells there is strong negative feedback of glucose 6-phosphate (G6P) on hexokinase, the first enzyme of the head section of glycolysis[22]. In addition to feedback by G6P, feedback by FBP has also been reported in Ehrlich ascites tumor cells[23]. The feedback control on the head section of glycolysis by downstream intermediates shows a clear time delay and affects the glycolytic rate in the head section with a half time of order 10 s[24,25]. Binding of G6P to hexokinase also may lead to translocation of this enzyme with a similar time course[26]. The delayed negative feedback from the PGI pool on hexokinase is represented in the present model by a second order reaction of PGI with the head section, governed by a second order forward rate constant and a first order backward rate constant (see Eq. 22 in Supplementary Text). The forward reaction inactivates the head section and the backward reaction reactivates the inactivated head section. Representation in this simple form adequately describes the time delay of activation and reactivation. The activation state of the head section is represented by the active fraction, F_{active}. The delay in inhibition of the head section reproduces the overshoot in FBP concentration after glucose addition to the cell suspension, whereas previously ATP trapping in the mitochondria[7,9] or complex regulatory interactions between two compartmentalized glycolytic systems had to be hypothesized[16] to account for the time course of glucose uptake and FBP.

The tail section of glycolysis in the model is downstream of the FBP pool. It consists of the glycolytic enzymes aldolase, triose phosphate isomerase, glyceraldehyde 3-phosphate dehydrogenase (GAPDH), phosphoglycerate kinase, phosphoglycerate mutase, enolase and pyruvate kinase. Input reactants for the tail section are FBP, NAD^+, ADP and inorganic phosphate (P_i), while its products are pyruvate, NADH and ATP. Equation 2 in the Supplementary Text represents the tail section in a lumped fashion. Each reactant which influences the reaction rate is represented by a Michaelis-Menten constant, while NADH, which is a product of the GAPDH reaction, negatively affects the forward net reaction rate in the tail section[21,27].

The equation for the lactate dehydrogenase equation, pyruvate + NADH ⇌ lactate + NAD^+, was taken from Lambeth and Kushmerick[28]. ATP consumption for maintenance, growth and cell function correlates linearly with the fall in adenine

nucleotide concentration (ATP+ADP) in the experimental data, as found in the experiments of Figure 2. Incorporating this relation in the model reproduces the steep decline in ATP hydrolysis which was found after acutely giving glucose to cells which had been deprived of glucose for some time.

The equations determining rates of change of metabolite levels represent balances for key players in the model: the balance of phosphoryl groups in the ATP, ADP and FBP pools, which play a central role in energy metabolism; the balance of carbon metabolites representing the distribution and storage of glucose; the balance of reduction of NAD to NADH and the reverse oxidation reaction, i.e. the NADH/NAD redox balance.

The present model provides only a coarse representation of regulatory mechanisms active *in vivo*, but it fulfills the goal of reproducing a broad range of measurements on EATC, both the average glucose and oxygen uptake measurements during 1 hour in Warburg's laboratory[5,6], as well as kinetic responses of glucose and oxygen uptake, lactate production, FBP and ATP levels measured in the first seconds and minutes following glucose addition[7,29–32]. The model is subsequently used to investigate what the physiological role is of high expression levels of glycolytic enzymes for the survival and growth of cancer cells.

The model equations are all given in the Supplementary Text, where the assumptions underlying the model are discussed further. The computational methods for integrating the system of ordinary differential equations, for parameter estimation and for uncertainty analysis are also given in the Supplementary Text.

Results

Model analysis of kinetic data on ascites tumor cell suspensions *in vitro*

A data set was assembled consisting of representative experiments from the literature to be used to estimate parameters

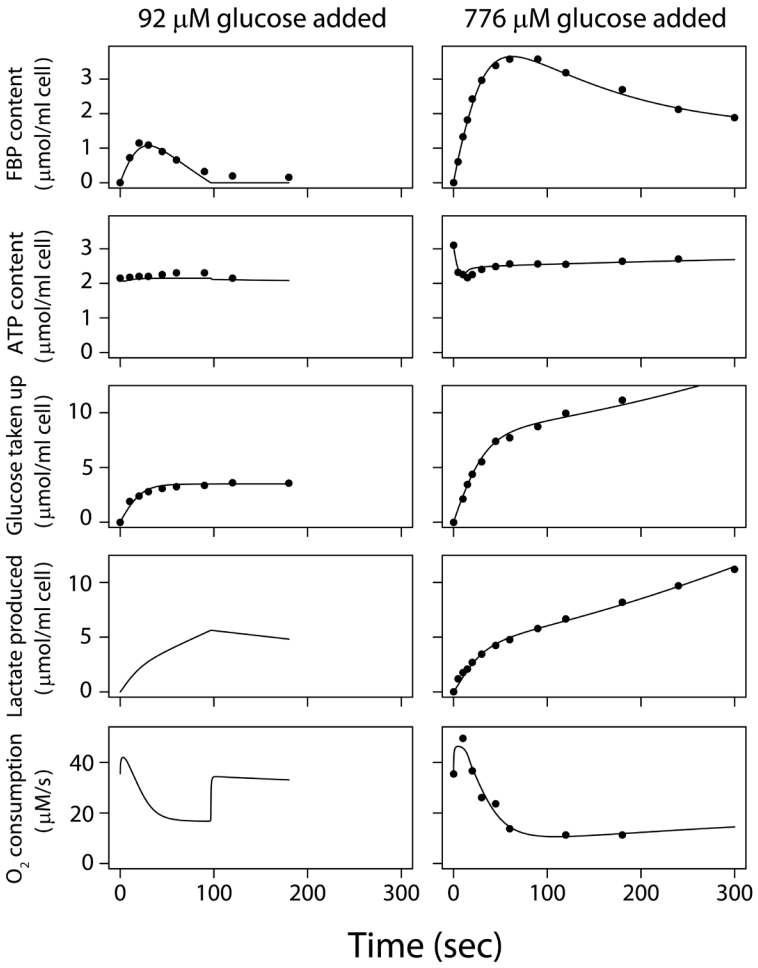

Figure 2. Response of Ehrlich ascites tumor cells *in vitro* to addition of different amounts of glucose. Glucose concentration was zero at t<0, and the cells respired on endogenous substrates, such as lactate. Glucose was added at t=0. Data for experiments (dots) and model fit (lines). Left hand column: low initial glucose concentration (92 µM) was added at t=0 to a suspension of 2.2 volume percent tumor cells. Right hand column: a higher glucose concentration (776 µM) was added at t=0 to a suspension of 2.9 volume percent tumor cells. Contents of fructose 1,6-bisphosphate (FBP), ATP, total glucose taken up and total lactate produced since t=0 are given in µmol/ml cell volume. The rate of O_2 consumption is given in µmol/liter intracellular water/sec.

for the model of metabolic responses of Ehrlich ascites tumor cells (see Supplementary Text). The data sets are exemplary, but they are representative of results measured in many laboratories[6–8,16,29–41]. All selected experiments were done at 37°C on Ehrlich ascites cells that had been grown in mice. During the experiments, aerated tumor cell suspensions were diluted in buffer solution. Cells and suspension had been depleted of glucose for some time and were respiring on endogenous substrates such as lactate, which was abundantly present. At t=0, glucose was added to the suspension. Two kinetic data sets for the first 3–5 min consist of responses to addition of 92 µM and 776 µM glucose to cells which had been grown in ascites fluid in mice and suspended in media without glucose.

These measured responses of glucose-depleted EATC to addition of low concentrations of glucose are shown in Figure 2. The model is calibrated (Supplementary Text) on these data sets[8,32], which are representative of results in several laboratories[7,29–31,39,41]. After adding 92 µM glucose initially[32], glucose was soon exhausted (Dataset 1, experiment 1)[42]. After adding 776 µM glucose[8], the glucose uptake rate was ~295 µM/s initially and lactate production rose to 157 µM/s in 5 s (Dataset 1, experiment 2)[42]. Glucose uptake was subsequently reduced by >90% within 90 s[7,8,30,39]. According to the model, this decline is caused by delayed feedback inhibition on the head section of glycolysis.

During the first 20 s mitochondrial respiration is stimulated (Figure 2, right); after 30 s respiration is reduced appreciably below the initial value found before glucose addition[7,29]. Both the simulation and direct calculation of the mass balance of the measured phosphate metabolites shows a ~70% decline in ATP hydrolysis in the first minute, correlating with the amount of ATP plus ADP broken down to AMP, adenosine, inosine etc. This breakdown is reflected in the decreased ATP level after glucose addition (Figure 2, right). After the initial breakdown, adenine nucleotide levels recover in 0.5–1 hour[27,43]. The reduction of respiration after glucose addition is initially strongly determined by the reduced ATP hydrolysis.

Half of the glucose taken up in the first minute after addition is stored as PGI, mainly FBP. Subsequently, FBP declines (Figure 2, right), reflecting the delayed negative feedback on the head section of glycolysis, and settles at still appreciable levels. At 5 minutes after glucose addition, 18% of the total glucose taken up is found intracellularly as PGI, 43% has been excreted as lactate and 34% is stored intracellularly in other forms, e.g. glycogen, nucleosides and amino acids.

Model predictions were subsequently compared with experiments not used for parameter estimation (Supplementary Text): Warburg's laboratory measured 63±14 (SD) µM/s lactate production and 19±7 µM/s O_2 consumption in EATC during 1 hour aerobic incubation with glucose[6]; the simulation predicts 52.5 µM/s lactate production and 19.8 µM/s oxygen consumption (Dataset 1; exp 3)[42]. Simulation further predicts that lactate production is increased by 61% during anoxia (Pasteur effect; Dataset 2)[44]; for comparison, in Warburg's laboratory lactate production increased by 61±32% (SD) when oxidative phosphorylation was blocked[6]. Above 200 µM added glucose concentration, the peak FBP content levels off, both in experiments[32,45] and *in silico* (Dataset 1, experiment 4)[42]. This is consistent with the estimated $K_{m,glucose}$ of 51 µM for the head section (Supplementary Table 3) and $K_{m,glucose}$ values reported for hexokinase, 46–78 µM[20]. The fast FBP and lactate accumulations measured at 5 and 10 sec[8,45] after glucose addition agree with the simulations: tumor cells store for instance ~700 µM FBP intracellularly in 10 s if the initial extracellular glucose concentration is merely 77 µM (Dataset 1, experiment 5)[42], demonstrating their high capacity to seize glucose.

The simulations reproduce the persistent inhibition of respiration by glucose, known as the Crabtree effect[14]: the average reduction over 1 hour after adding 11 mM glucose is 44% (Dataset 1, experiment 3)[42], while a 30±12% (SD) reduction was measured in Warburg's laboratory[6]. While the decline of respiration in the first minutes after glucose addition (Figure 2) is mainly caused by reduced ATP hydrolysis, the persisting high glycolytic ATP synthesis[6] continues to keep ADP concentration and respiration reduced much longer (Dataset 1: exp 3)[42].

Simulations predict that ATP levels decline by 30% after glucose addition at low pyruvate concentrations because of breakdown to AMP, inosine etc. (Figure 2), but when 5 mM pyruvate is added, the predicted decline of ATP is merely 0.1% and the FBP peak decreases by 21% (Dataset 3)[46]; a similar pattern is seen experimentally[27].

In short, the present small model economically integrates experimental data and biochemical knowledge, and quantitatively reproduces experimental results on the Warburg effect, Pasteur effect, Crabtree effect and kinetic experiments with addition of glucose. The model simulations show that after a period of glucose depletion, glucose uptake is much faster than measured for the steady Warburg effect, and that fructose 1,6-bisphosphate accumulates and can be quickly taken up in the cell's biomass and consumed by the tail end of glycolysis where ATP is synthesized. This time-course is the consequence of inhibition of the head section of glycolysis in about 1 minute when glycolytic intermediates accumulate, and slow disinhibition of the glycolytic head section when glycolytic intermediate levels are low. A second mechanism for energy homeostasis suggested by the model consists of reduction of ATP usage, and underlies the first phase of the Crabtree effect.

Prediction of the function of the dynamic metabolic regulation in the tumor cell

Next the role that the dynamic regulatory mechanisms captured in the computational model may play in tumor cell physiology is considered. ATP synthesis during hypoxia has long been considered a possible role for the glycolytic system underlying the Warburg effect. The O_2 saturation of hemoglobin in capillaries in tumor tissue is often low or zero[47]. O_2 concentrations are low in tumor tissue[48] as well as in the ascites fluid in mice where EATC were grown[5]. Tumor blood flow sometimes stops temporarily[49] and many blood vessels are not perfused over

extensive periods[50]. Fluctuations in tumor blood flow may lead to cycling hypoxia[11,51] and periodic glucose shortages. If O_2 is still available when glucose is depleted, ATP can be synthesized by oxidative phosphorylation, burning lactate, fatty acids or glutamine[52]. If glucose is still present, glycolysis can synthesize ATP if O_2 is depleted; however, the environment in solid tumors contains a glucose concentration in the order of a few hundred μM, and in many cases even <100 μM[53]. Cells die when anoxia is combined with glucose depletion for substantial periods of time[1]. Figure 2 suggests that tumor cells can store FBP and other PGI during periods of sufficient glucose supply during high blood flow in tissue ("times of abundance"). Periods of low blood flow lead to depletion of O_2 and glucose ("times of famine"), and the cells can then use the stored PGI to synthesize ATP. For each FBP molecule metabolized in the tail part of glycolysis, 4 ATP molecules are synthesized (Figure 1). Stored FBP can reach ≥5000 μM, with additionally ≥1200 μM 6-carbon units stored as other PGI species (Dataset 1)[42]. This enables the synthesis of at least 4 × (5000+1200) μM = 25 mM ATP from PGI, potentially sustaining a high rate of ATP hydrolysis in EATC for >2 min, even after glucose and oxygen are depleted. The reduction of ATP consumption in the model, also seen experimentally *in vitro*, provides an additional protective mechanism: protein, DNA and RNA synthesis are presumably reduced first when ATP levels fall, followed by sodium and calcium ion pumping[54–57]. Warburg established experimentally that one-fifth of the normal growth energy supplied for 24 hours preserved the transplantability of tumor cells[1]. Reduced ATP hydrolysis required for maintaining cell viability may therefore be supported much longer than 2 min (probably at least 10 min) from FBP and other PGI stores.

The functioning of the FPB storage system of tumor cells is difficult to study experimentally *in vivo*. This may require metabolic measurements at a spatial resolution sufficient to distinguish low and high glycolytic cells. High time resolution to resolve the transient metabolic responses and experimental control of fluctuating O_2 and nutrient supply is probably also needed. While experimental tests are challenging, the functioning of dynamic glycolytic regulation in tissue may be investigated with computational simulation.

Simulating tumor cell metabolism during oxygen and glucose fluctuations in tissue

There are limitations to experimental approaches, but the functioning of FBP buffering *in vivo* can be predicted with the present metabolic model, extended with well-known equations for glucose and O_2 transport by blood flow and diffusion to simulate tumor tissue (Supplementary Text). The model equations for tissue transport are described in the Supplementary Text. Figure 3 shows a simulation of a hypothetical situation in tissue with blood flow fluctuating around a low average value. Similar fluctuations in blood flow are common in tumor tissue[10,11,49–51]. Blood flow rate, diffusion distance and plasma metabolite concentrations were set to values found in experiments on tumors implanted in rats[58], while the metabolic characteristics of the simulated cells are set as determined in EATC *in vitro* (see above). O_2 and glucose concentrations become virtually zero during the low blood flow phase, and the head section of glycolysis (Figure 3, dashed curve) and oxidative phosphorylation (blue curve) both stop. ATP synthesis from the stored FBP is quickly upregulated to replace reduced oxidative phosphorylation (red curve) and keeps ATP levels and ATP synthesis virtually constant near the level found at constant high blood flow (Dataset 4a)[59]. The effect of ATP synthesis by the FBP buffer mechanism is investigated by uncoupling glycolytic flux in the tail section from the associated phosphorylation of ADP. This uncoupling leads to an immediate decrease in adenine nucleotide levels and ATP hydrolysis is subsequently reduced, owing to the second homeostatic mechanism in the model. This prevents progressive imbalance of ATP hydrolysis and consumption, albeit at a lower turnover rate.

The transition from constant to cycling blood flow was simulated (Figure 4 and Dataset 4b)[59], with 80% of the cell volume consisting of tumor cells with full glycolytic capacity while the remaining 20% consists of cells with glycolytic capacity reduced to 10%. As long as blood flow is constant, ATP levels and ATP hydrolysis for cell functioning are maintained in both cell types. When blood flow starts to fluctuate, ATP concentration and ATP usage are well maintained in the cells with full glycolytic capacity. However, in the cells with 10% of the tumor glycolytic capacity, FBP buffering is appreciably decreased and adenine nucleotide levels and ATP hydrolysis fall quickly after blood flow fluctuations start. The low-capacity glycolytic cells sustain a lower rate of ATP turnover during cycling blood flow. Uncertainty analysis shows that the model predictions are sufficiently constrained (Supplementary Figure 1, Supplementary Figure 2 and Supplementary Text)[60].

ATP turnover was well maintained at a constant blood flow, even for cells at merely 1.5% of the tumor glycolytic capacity which are representative of many normal cell types (Supplementary Figure 3 and Dataset 4c)[1,59]. However, FBP buffering was weak and ATP turnover strongly decreased during blood flow cycling. Cells at full tumor glycolytic capacity take up 50 μM/s glucose averaged over a flow cycle, while cells at 1.5% glycolytic capacity take up only 2 μM/s glucose. ATP synthesis from the FBP buffer is very low and the storage of glucose-derived metabolites for growth is compromised. Tumor cells with high glycolytic capacity take much more than their fair share of glucose.

The response to cycling blood flow in Figure 4 is influenced by two homeostatic mechanisms: FBP buffering and adaptation of ATP turnover. If ATP hydrolysis is made insensitive to the cell's adenine nucleotide status and adaptation of ATP turnover therefore ineffective, the FBP buffering mechanism alone can still prevent the collapse of ATP during blood flow stops if the full tumor glycolytic capacity is active in the simulation (see Supplementary Figure 4 and Supplementary Text). However, glycolytic capacity reduction below the tumor level leads to compromised ATP concentration and ATP hydrolysis during flow stops. PGI stores accumulated in highly glycolytic cells during

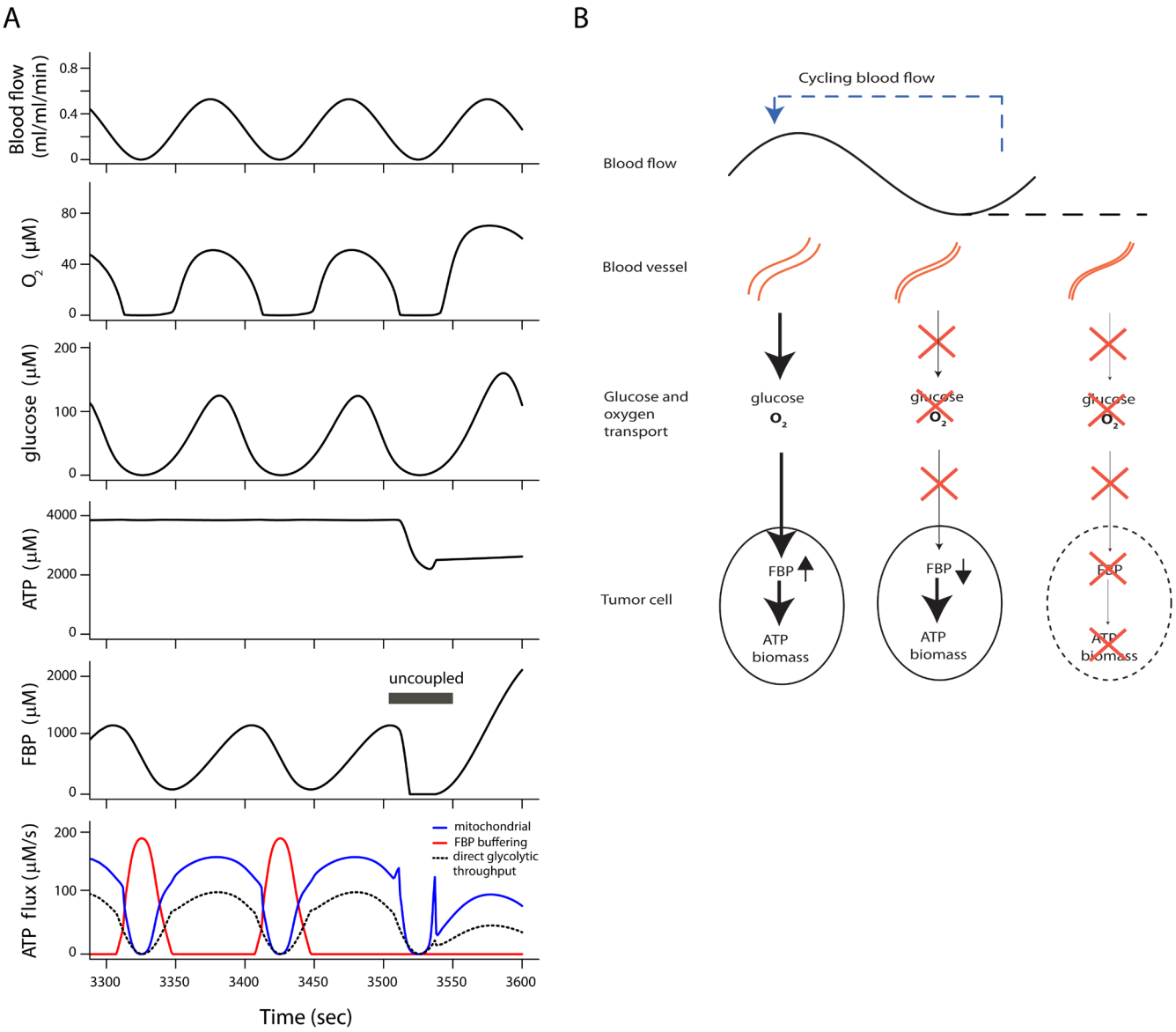

Figure 3. Tumor cell metabolism in tissue during cycling blood flow. (**A**) Model simulation of tumor cell metabolism in tissue during cycling blood flow, demonstrating ATP synthesis buffered from fructose 1,6-bisphosphate (FBP) stores. All cells have the full tumor glycolytic capacity. ATP synthesis by oxidative phosphorylation (blue line) fails periodically during low blood flow because of low oxygen supply. Glycolytic ATP synthesis by direct throughput of FBP from head to tail section fails because of glucose depletion (dashed black line). A burst of ATP synthesis from the stored fructose 1,6-bisphosphate (FBP) and other phosphorylated glycolytic intermediates (red curve) maintains ATP levels during glucose and O_2 shortages. A steady state was reached after the transition at t=0 to cycling blood flow. ATP synthesis from decreasing levels of FBP was uncoupled between 3505 and 3550 seconds, leading to an immediate fall in ATP level. (**B**) Scheme of energy and nutrient buffering during fluctuating O_2 and glucose supply. During high blood flow, FBP and other phosphorylated glycolytic intermediates are stored in the tumor cells. At low blood flow glucose and O_2 are depleted. Flux in the tail part of glycolysis is maintained by use of previously stored FBP, which is replenished if blood flow increases. If blood flow stops for a long time, the intracellular FBP store is depleted.

periods of high blood flow are often several-fold larger than maximal tissue glucose content (Dataset 5)[61], which underscores their importance for energy and nutrient buffering.

These simulations address conditions in tumor tissue with cycling hypoxia and nutrient shortages caused by cycling blood flow. In the next section it is considered how hypoxia and low glucose concentrations can also be caused by large diffusion distances in the ascites fluid in the murine peritoneal cavity in which the ascites cells were grown in the laboratories of Warburg[6], Chance[29], Coe[32] and others.

Simulating oxygen and glucose diffusion in ascites fluid containing tumor cells

Warburg observed that glucose and O_2 concentrations were very low in the ascites fluid in the abdomen of mice in which

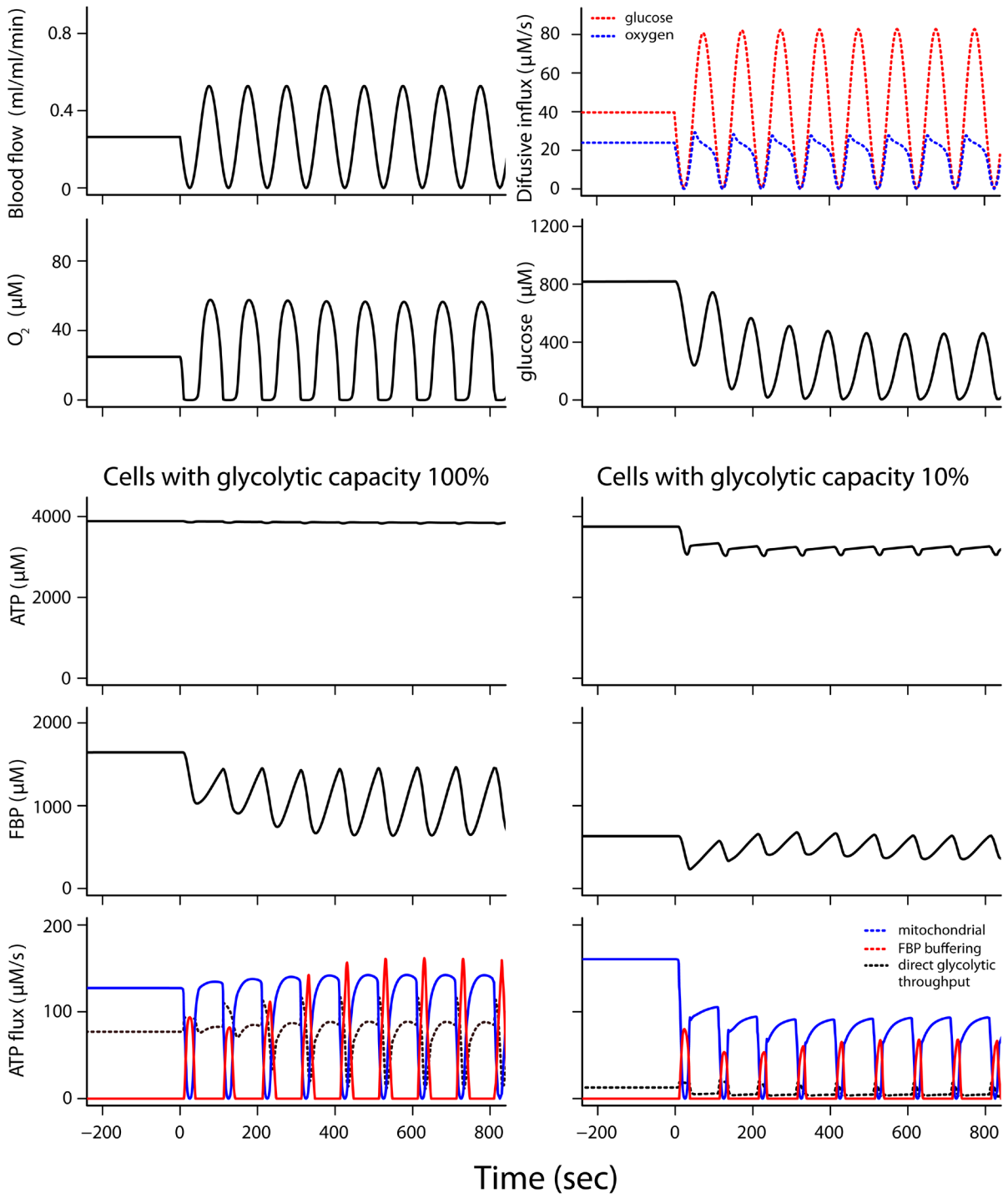

Figure 4. Simulations predicting tumor tissue metabolism during the start of blood flow cycling. In this simulation, 80% of the cell volume had the full tumor glycolytic capacity; 20% of the cell volume had 10% of the full glycolytic capacity. The two top rows show tissue conditions experienced by both cell types. Blood flow and diffusion flux of glucose and O_2 from the microvessel into tissue are given (top row). O_2 and glucose concentrations seen by both cell types are given in the second row. Simulation for cells ~18 µm from the microvessel. High ATP consumption, >160 µM/s, was maintained at constant blood flow. See legend to Figure 3 for description of ATP synthesis fluxes. When blood flow started to fluctuate at t=0, ATP synthesis from the decline in stored fructose 1,6-bisphosphate (FBP) and other phosphorylated glycolytic intermediates (red curve) maintained ATP levels and high ATP hydrolysis rates in cells with full tumor glycolytic capacity; however, there was a drop in ATP level and ATP hydrolysis rate in the cells with reduced glycolytic capacity.

he was growing EATC at a high cell density[5]; others reported ~300 µM glucose in this environment[62–64]. These low glucose concentrations are still sufficient for virtually maximal glucose consumption by EATC; however, glucose diffusion into the ascites fluid measured *in vivo* has limited capacity[62], so that it can provide only a small fraction of this maximal consumption. Simulations of EATC in ascites fluid with the present model provide an explanation for this paradox: diffusion gradients over distances of hundreds of µm cause the glucose concentration in most of the ascites fluid in the peritoneal cavity to be far below the average concentration measured in fluid samples (Dataset 6, Dataset 7)[65,66]. Details of the calculation and results are given in the Supplementary Text. It is therefore plausible that most tumor cells in the peritoneal cavity are exposed to low glucose concentrations and consequently have very low metabolic rates.

Tumor cells in the ascites fluid shift position because of body movements and intestinal peristalsis[64] which leads to quick changes in O_2 and glucose concentrations. The cells are therefore exposed to fluctuating high and low nutrient concentrations (Supplementary Text). Greedy glucose uptake followed by storage of glucose-derived metabolites and buffering of ATP by a high-capacity glycolytic system may provide selective advantages to highly glycolytic tumor cells proliferating in environments with low and fluctuating glucose supply such as ascites fluid. This may favor the evolution of a high-capacity dynamically regulated glycolytic system in the tumor cells. Similar consideration may apply to cells in solid tumor environments which also often show low and fluctuating oxygen and nutrient supply.

Dataset 1. Model simulation results for 5 experiments on suspensions of Ehrlich ascites tumor cells *in vitro*

http://dx.doi.org/10.5256/f1000research.15635.d212544

Experiment 1: low glucose concentration added (92 µM); Experiment 2: higher glucose concentration added (776 µM); Experiment 3: one hour aerobic incubation with high concentration of glucose (11.1 mM); Experiment 4: maximum FBP content following addition of a range of glucose amounts; Experiment 5: accumulation of lactate and FBP after 5 and 10 s at two low initial glucose levels; Experiments 1–5 are described in Supplementary Text: Calibrating the computational model with experimental data.

Dataset 2. Simulation results of incubation of Ehrlich ascites tumor cells at 11 mM glucose without oxygen, simulating experiments in Warburg's laboratory

http://dx.doi.org/10.5256/f1000research.15635.d212545

See description Experiment 6 in Supplementary Text: Testing the computational model with additional experimental data.

Dataset 3. Simulation results of incubation of Ehrlich ascites tumor cells *in vitro* with 5 mM pyruvate and 10 mM glucose

http://dx.doi.org/10.5256/f1000research.15635.d212546

See description of Experiment 7 in Supplementary Text: Testing the computational model with additional experimental data.

Dataset 4. Simulations of tumor tissue including fluctuating blood flow, diffusion and tumor cell metabolism

http://dx.doi.org/10.5256/f1000research.15635.d212547

ATP hydrolysis is high initially and strongly reduced when energy status is compromised. Simulation for tissue with a maximal diffusion distance of 40 µm. Result for the tissue layer at 15–20 µm from the blood vessel is given. Blood flow is constant for t≤0 and starts to fluctuate sinusoidally at t=0, periodically reaching zero for a moment, but not fully stopping.

For t ≤ 0: blood flow = offset.

For t>0: blood flow = offset - amplitude · sin(2πt/Tperiod).

offset = 4.4 ml/l intracellular H2O/s, amplitude = 4.4 ml/l/s, flow ≥ 0.

Worksheet A. Simulations of tumor cells (100% of cell volume at 100% of the glycolytic capacity). From 3505–3550 sec the contribution to ATP synthesis in the tail part of glycolysis derived from falling stores of fructose 1,6-biphosphate (FBP) and other GPI is uncoupled and therefore not contributing to total ATP synthesis.

Worksheet B. Simulations of tumor cells (80% of cell volume) and a second cell type with 10% of tumor glycolytic capacity (20% of volume) in tissue with fluctuating blood flow.

Worksheet C. Simulations of tumor cells (80% of cell volume) and a second cell type with 1.5% of tumor glycolytic capacity (20% of volume) in tissue with fluctuating blood flow.

See Supplementary Text for details.

Dataset 5. Simulations of tumor tissue with metabolism, diffusion and fluctuating low blood flow with long flow stops

http://dx.doi.org/10.5256/f1000research.15635.d212548

Maximal ATP hydrolysis 100 µM/s. In the second ("Glycolytic capacity 100%") and penultimate ("FBP buffering uncoupled") worksheet all cells had the full glycolytic capacity of tumor cells. In the rest of the simulations, 95% of cell volume is occupied by tumor cells with glycolytic capacity at 100% of tumor cell level. A second cell type with lower glycolytic capacity occupies the remaining 5% of cell volume. Simulation for 8 tissue layers of width 5 µm, resulting in a maximal diffusion distance of 40 µm. Result is given for the tissue layer at 15–20 µm from the blood vessel.

Blood flow is constant for t≤0 and starts to fluctuate sinusoidally at t=0, periodically stopping fully for ~2 min; for t ≤ 0: blood flow = offset; for t>0: blood flow = offset - amplitude · sin(2ππ/Tperiod).

offset = 2.2 ml/l intracellular H2O/s, amplitude = 3.5 ml/l/s, flow ≥ 0.

Six different simulations with different glycolytic capacities in the second cell type are given.

Worksheet "Glycolytic capacity 100%": all cells 100% of tumor cell level; worksheet "Glycolytic capacity 50%": Second cell type: glycolytic capacity 50% of tumor cell level; worksheet "Glycolytic capacity 30%": Second cell type: glycolytic capacity 30% of tumor cell level; worksheet "Glycolytic capacity 10%": Second cell type: glycolytic capacity 10% of tumor cell level; worksheet "Glycolytic capacity 1.5%": Second cell type: glycolytic capacity 1.5% of tumor cell level; worksheet "FBP buffering uncoupled": Glycolytic ATP synthesis depending on falling stores of fructose 1,6-biphosphate (FBP) and other GPI uncoupled, glycolytic capacity 100% of tumor level for all cells; worksheet "Parameters": the parameters representing the glycolytic capacities in the simulations above.

Dataset 6. Simulation of diffusion of glucose from the peritoneum into ascites fluid not containing cells during 3 min

http://dx.doi.org/10.5256/f1000research.15635.d212549

An experiment by Kemp and Mendel is simulated[62], see Supplementary Text. Tumor cells and metabolism were absent in this simulation. The injected ascites fluid initially contained 167 µM glucose and the time course of glucose concentrations was simulated in sixty three stacked fluid layers with an increment of 10 µm per layer.

Dataset 7. Simulation of steady-state diffusion gradients in a suspension of Ehrlich ascites tumor cells (25% vol/vol) in ascites fluid in the peritoneal cavity

http://dx.doi.org/10.5256/f1000research.15635.d212550

This simulates conditions under which Erhlich ascites cells were grown in Warburg's laboratory[5,6] with a maximal diffusion distance of 630 µm from blood vessel into ascites fluid. This simulation resolves a paradox discussed by Kemp and Mendel[62]. Sixty three layers of ascites fluid with a radius increment of 10 µm per layer were simulated.

Discussion

The present small computational model reproduces the three effects named after Warburg, Pasteur and Crabtree, respectively, which persist for an hour or more; at the same time the model captures the kinetic behavior in the first minutes after glucose addition and it is consistent with biochemical knowledge. This new concise model gives a new, testable explanation of the dynamic behavior of tumor cell metabolism, replacing the model of Chance and Hess[7,9]. Although the latter model has large historical value as the first digital model of a biochemical system, it contains assumptions which are biochemically untenable. Despite the present model's explanation of a broad range of *in vitro* experimental data, further testing and refinement is necessary. Better understanding of the differential regulation of the head and tail sections of glycolysis is desirable. This requires experimental data revealing how the duration and extent of glucose depletion and the concentration of glycolytic intermediates affect the dynamic regulation of the head section of glycolysis in tumor cells. Although the details of the model deserve further investigation, it represents the experimental responses of ascites tumor metabolism in terms of glucose uptake, lactate production, FBP accumulation and ATP synthesis well.

The decrease of ATP consumption, correlating with the change in adenine nucleotide pool status (ATP+ADP), is required to fit the measured data in Figure 2. It should be noted that the decrease in ATP+ADP corresponds quantitatively with the accumulation of AMP, inosine, adenosine etc.[27,43]. The mechanism of this decrease of ATP hydrolysis requires further investigation. A useful extension would further be to model how the breakdown of ADP to AMP, inosine etc. helps to maintain the free energy of ATP hydrolysis under energetic stress by increasing the ATP/ADP ratio[27,67].

The model predicts the metabolic responses in the tissue situation and provides a plausible and testable explanation why tumor cells benefit from a dynamically regulated uptake capacity of glucose that exceeds the requirements of the steady Warburg effect. The model predicts that tumor cells in tissue efficiently gulp glucose at low extracellular concentrations, and store it for the dynamic buffering of ATP and nutrients during periods of low blood flow. The model predicts that the high glucose-gulping capacity is ready for immediate action during times of famine, and is partially inhibited with some delay during times of feast, presumably to prevent overloading of the tumor cells with glucose products, while providing a time window of high uptake capacity. A remaining question is whether the time window, which provides a high capacity of glucose uptake provided by balance of inhibition and disinhibition of the head section of glycolysis, may be optimal for some cycling blood flow frequencies and not for others.

Experimental interventions in the dynamic regulation of the head section of glycolysis may be employed to test the importance of the dynamic regulatory mechanism for tumor cell proliferation and growth. It is conceivable that such interventions could be beneficial for the treatment of tumors, limiting the competitiveness of tumor cells against normal tissue and immune cells.

When tumor cells have been deprived of glucose for some time and are subsequently exposed to glucose, they can invest ~600 µM/s ATP for many seconds to sequester glucose (Dataset 1)[42]. For comparison, human vastus lateralis muscle consumes ~1000 µM/s for 6 s during maximal sprint performance[68]. The high glucose uptake capacity of tumor cells tends to keep tissue glucose concentrations low, making it difficult for competing cells with a lower glucose uptake capacity to take up sufficient glucose when supply is low and fluctuating. This may be the driving force for the evolution of Ehrlich ascites cells and tumor cells evolving in solid tumors to a state with high and dynamically regulated glucose metabolic uptake. Cells with higher glycolytic capacity also maintain higher levels of phosphorylated glycolytic intermediates to provide building blocks for macromolecular synthesis and cell growth, in addition to the dynamic ATP buffering. The hypothesis is therefore put forward here that the nutritional and energetic buffering mediated by dynamic regulation of high-capacity glucose metabolism by the glycolytic chain may give tumor cells a selective advantage over cells with lower glycolytic capacity under conditions of fluctuating oxygen and glucose supply.

Data availability

Dataset 1. Model simulation results for 5 experiments on suspensions of Ehrlich ascites tumor cells *in vitro*. Experiment 1: low glucose concentration added (92 µM); Experiment 2: higher glucose concentration added (776 µM); Experiment 3: one hour aerobic incubation with high concentration of glucose (11.1 mM); Experiment 4: maximum FBP content following addition of a range of glucose amounts; Experiment 5: accumulation of lactate and FBP after 5 and 10 s at two low initial glucose levels; Experiments 1–5 are described in Supplementary Text: Calibrating the computational model with experimental data. DOI: https://doi.org/10.5256/f1000research.15635.d212544[42].

Dataset 2. Simulation results of incubation of Ehrlich ascites tumor cells at 11 mM glucose without oxygen, simulating experiments in Warburg's laboratory. See description

Experiment 6 in Supplementary Text: Testing the computational model with additional experimental data. DOI: https://doi.org/10.5256/f1000research.15635.d212545[44].

Dataset 3. Simulation results of incubation of Ehrlich ascites tumor cells *in vitro* with 5 mM pyruvate and 10 mM glucose. See description of Experiment 7 in Supplementary Text: Testing the computational model with additional experimental data. DOI: https://doi.org/10.5256/f1000research.15635.d212546[46].

Dataset 4. Simulations of tumor tissue including fluctuating blood flow, diffusion and tumor cell metabolism. ATP hydrolysis is high initially and strongly reduced when energy status is compromised. Simulation for tissue with a maximal diffusion distance of 40 µm. Result for the tissue layer at 15–20 µm from the blood vessel is given. Blood flow is constant for t≤0 and starts to fluctuate sinusoidally at t=0, periodically reaching zero for a moment, but not fully stopping.

For t ≤ 0: blood flow = offset.

For t>0: blood flow = offset - amplitude · sin(2πt/Tperiod).

offset = 4.4 ml/l intracellular H_2O/s, amplitude = 4.4 ml/l/s, flow ≥ 0.

Worksheet A. Simulations of tumor cells (100% of cell volume at 100% of the glycolytic capacity). From 3505–3550 sec the contribution to ATP synthesis in the tail part of glycolysis derived from falling stores of fructose 1,6-biphosphate (FBP) and other GPI is uncoupled and therefore not contributing to total ATP synthesis.

Worksheet B. Simulations of tumor cells (80% of cell volume) and a second cell type with 10% of tumor glycolytic capacity (20% of volume) in tissue with fluctuating blood flow.

Worksheet C. Simulations of tumor cells (80% of cell volume) and a second cell type with 1.5% of tumor glycolytic capacity (20% of volume) in tissue with fluctuating blood flow.

See Supplementary Text for details. DOI: https://doi.org/10.5256/f1000research.15635.d212547[59].

Dataset 5. Simulations of tumor tissue with metabolism, diffusion and fluctuating low blood flow with long flow stops. Maximal ATP hydrolysis 100 µM/s. In the second ("Glycolytic capacity 100%") and penultimate ("FBP buffering uncoupled") worksheet all cells had the full glycolytic capacity of tumor cells. In the rest of the simulations, 95% of cell volume is occupied by tumor cells with glycolytic capacity at 100% of tumor cell level. A second cell type with lower glycolytic capacity occupies the remaining 5% of cell volume. Simulation for 8 tissue layers of width 5 µm, resulting in a maximal diffusion distance of 40 µm. Result is given for the tissue layer at 15–20 µm from the blood vessel.

Blood flow is constant for t≤0 and starts to fluctuate sinusoidally at t=0, periodically stopping fully for ~2 min; for t ≤ 0: blood flow = offset; for t>0: blood flow = offset - amplitude · sin(2πt/Tperiod).

offset = 2.2 ml/l intracellular H_2O/s, amplitude = 3.5 ml/l/s, flow ≥ 0.

Six different simulations with different glycolytic capacities in the second cell type are given.

Worksheet "Glycolytic capacity 100%": all cells 100% of tumor cell level; worksheet "Glycolytic capacity 50%": Second cell type: glycolytic capacity 50% of tumor cell level; worksheet "Glycolytic capacity 30%": Second cell type: glycolytic capacity 30% of tumor cell level; worksheet "Glycolytic capacity 10%": Second cell type: glycolytic capacity 10% of tumor cell level; worksheet "Glycolytic capacity 1.5%": Second cell type: glycolytic capacity 1.5% of tumor cell level; worksheet "FBP buffering uncoupled": Glycolytic ATP synthesis depending on falling stores of fructose 1,6-biphosphate (FBP) and other GPI uncoupled, glycolytic capacity 100% of tumor level for all cells; worksheet "Parameters": the parameters representing the glycolytic capacities in the simulations above. DOI: https://doi.org/10.5256/f1000research.15635.d212548[61].

Dataset 6. Simulation of diffusion of glucose from the peritoneum into ascites fluid not containing cells during 3 min. An experiment by Kemp and Mendel is simulated[62], see Supplementary Text. Tumor cells and metabolism were absent in this simulation. The injected ascites fluid initially contained 167 µM glucose and the time course of glucose concentrations was simulated in sixty three stacked fluid layers with an increment of 10 µm per layer. DOI: https://doi.org/10.5256/f1000research.15635.d212549[65].

Dataset 7. Simulation of steady-state diffusion gradients in a suspension of Ehrlich ascites tumor cells (25% vol/vol) in ascites fluid in the peritoneal cavity. This simulates conditions under which Erhlich ascites cells were grown in Warburg's laboratory[5,6] with a maximal diffusion distance of 630 µm from blood vessel into ascites fluid. This simulation resolves a paradox discussed by Kemp and Mendel[62]. Sixty three layers of ascites fluid with a radius increment of 10 µm per layer were simulated. DOI: https://doi.org/10.5256/f1000research.15635.d212550[66].

Software availability

Source code available from: https://github.com/jhvanbeek/Metabolic-model-DSWE.

Archived source code at time of publication: http://doi.org/10.5281/zenodo.1322391[69].

Competing interests

No competing interests were disclosed.

Grant information

The author(s) declared that no grants were involved in supporting this work.

Acknowledgements

I thank SURFsara (https://www.surfsara.nl) for using the Lisa Compute Cluster where many of the computer calculations were performed.

Supplementary materials

Supplementary Text. Description of the computational model. This file also includes kinetic rate equations and differential equations for metabolite concentration changes with detailed description. In addition, it contains a description of the transport equations for oxygen and metabolites used for simulation of metabolism in tissue with cycling blood flow; also included are descriptions of computational methods, parameter optimization, analysis of prediction uncertainty, and of the experimental data sets used to calibrate and test the model. Description of simulation of cells growing in ascites fluid.

Click here to access the data.

Supplementary Figure 1. Uncertainty in prediction of the simulation results for tissue with cycling blood flow. The simulation in Figure 4 was repeated with parameter sets from 45 MCMC runs replicated with independent random seeds. The lines give the median (black) and the estimated 5 and 95% quantiles (red) of the prediction. This reveals the uncertainty in the model prediction of Figure 4. Model simulations are for tissue during blood flow cycling. Eighty percent of the cells had the full tumor glycolytic capacity (left column); 20% of the cell volume had 10% of the full glycolytic capacity (right column). The two top rows show tissue conditions experienced by both cell types. Blood flow was initially constant at 0.264 ml/ml intracellular H_2O/min. For t>0 a sinus wave with amplitude 0.264 ml/ml/min was superimposed. High ATP consumption, >160 μM/s, was maintained at constant blood flow. When blood flow started cycling at t=0, ATP synthesis from the decline in fructose 1,6-bisphosphate (FBP) and other phosphorylated glycolytic intermediates (bottom row) maintained ATP levels and ATP hydrolysis rates in cells with full tumor glycolytic capacity. However, there was a sharp drop in ATP levels and hydrolysis rate in the cells with reduced glycolytic capacity. The 5% and 95% quantiles show that the predicted response pattern is reproducible for a broad range of parameter sets which reflect the potential experimental variation in the data used for parameter optimization.

Click here to access the data.

Supplementary Figure 2. Variation in simulation results for the *in vitro* experiments (see Figure 2). The time courses were calculated using the final parameter sets from 45 MCMC ensembles, replicated with independent random seeds (same as in Supplementary Figure 1). All 45 results for individual parameter sets were plotted (blue lines). The time courses for the distinct parameters sets correspond within a narrow range.

Click here to access the data.

Supplementary Figure 3. Simulation with cells at low glycolytic capacity during the start of cycling blood flow. Simulation as in Figure 4, but with 20% of the cells at 1.5% (rather than 10%) of the full glycolytic capacity. Model simulations of tissue during cycling blood flow: 80% of the cell volume had the full tumor glycolytic capacity; 20% of the cells had 1.5% of the full capacity, representative of many normal body cell types. The two top rows show tissue conditions experienced by both cell types. Blood flow was constant at 0.264 ml/ml intracellular H_2O/min before t=0. For t>0 a sinus wave with amplitude 0.264 ml/ml intracellular H_2O/min was superimposed. High ATP consumption, >160 μM/s, was maintained at constant blood flow. Concentrations and fluxes at ~18 μm from the microvessel are given. See the legend of Figure 3 for description of ATP synthesis fluxes. When blood flow started to fluctuate, ATP synthesis from the decline in fructose 1,6-bisphosphate (FBP) and other phosphorylated glycolytic intermediates (red curve) maintained ATP levels and high ATP hydrolysis rates in cells with full tumor glycolytic capacity. By contrast, glycolytic fluxes were low and there was a sharp drop in ATP levels in the cells with reduced glycolytic capacity.

Click here to access the data.

Supplementary Figure 4. Simulations of tumor metabolism during cycling and stopping blood flow. In the simulation on the second row and the bottom row all cells had the full tumor glycolytic capacity. In the third through penultimate row ATP concentrations and fluxes are given for cells which had their glycolytic capacity changed to a percentage of the full tumor cell glycolytic capacity, as indicated above the rows. These cells with reduced glycolytic capacity constitute 5% of the total cell volume; the remaining 95% of the cells had the full tumor glycolytic capacity (100%). Results are calculated at ~38 μm from the blood vessel. Blood flow and fluxes of O_2 and glucose carried into the tissue by the arterial blood are common to all simulations (top row); the other rows each represent a separate simulation. Blood flow was initially constant and started to fluctuate at t=0, including flow stops. All ATP fluxes and blood flow are expressed per volume of intracellular H_2O. The ATP synthesis flux is partitioned in oxidative phosphorylation (blue) and two contributions by the tail section of glycolysis, with fructose 1,6-bisphospate (FBP) either directly fed from the head part of glycolysis (direct glycolytic throughput: dashed line) or taken from decreasing FBP stores (FBP buffering: red line). When ATP synthesis depending on phosphorylated glycolytic intermediate stores was uncoupled (bottom row), ATP levels collapsed during flow stops, although glycolytic capacity was 100% in all cells.

Click here to access the data.

Supplementary Table 1. State variables in the model of tumor cell metabolism.

Click here to access the data.

Supplementary Table 2. Metabolic fluxes in the model of tumor cell metabolism.

Click here to access the data.

Supplementary Table 3. Parameters in the model of tumor cell metabolism.

Click here to access the data.

References

1. Warburg O: **On the origin of cancer cells.** *Science.* 1956; **123**(3191): 309–314.
PubMed Abstract | Publisher Full Text
2. Schulze A, Harris AL: **How cancer metabolism is tuned for proliferation and vulnerable to disruption.** *Nature.* 2012; **491**(7424): 364–373.
PubMed Abstract | Publisher Full Text
3. Vander Heiden MG, Cantley LC, Thompson CB: **Understanding the Warburg effect: the metabolic requirements of cell proliferation.** *Science.* 2009; **324**(5930): 1029–1033.
PubMed Abstract | Publisher Full Text | Free Full Text
4. Mayers JR: **Metabolic markers as cancer clues.** *Science.* 2017; **358**(6368): 1265.
PubMed Abstract | Publisher Full Text
5. Warburg VO, Hiepler E: **Versuche mit Ascites-Tumorzellen.** *Z Naturforschung.* 1952; **7b**: 193–194.
Reference Source
6. Tiedemann H: **[The metabolism of the ascites tumor of the mouse].** *Z Gesamte Exp Med.* 1952; **119**(3): 272–279.
PubMed Abstract | Publisher Full Text
7. Chance B, Hess B: **Spectroscopic evidence of metabolic control.** *Science.* 1959; **129**(3350): 700–708.
PubMed Abstract | Publisher Full Text
8. Lee IY, Strunk RC, Coe EL: **Coordination among rate-limiting steps of glycolysis and respiration in intact ascites tumor cells.** *J Biol Chem.* 1967; **242**(9): 2021–2028.
PubMed Abstract
9. Chance B, Garfinkel D, Higgins J, *et al.*: **Metabolic control mechanisms. 5. A solution for the equations representing interaction between glycolysis and respiration in ascites tumor cells.** *J Biol Chem.* 1960; **235**: 2426–2439.
PubMed Abstract
10. Dewhirst MW, Cao Y, Moeller B: **Cycling hypoxia and free radicals regulate angiogenesis and radiotherapy response.** *Nat Rev Cancer.* 2008; **8**(6): 425–437.
PubMed Abstract | Publisher Full Text | Free Full Text
11. Dewhirst MW: **Relationships between cycling hypoxia, HIF-1, angiogenesis and oxidative stress.** *Radiat Res.* 2009; **172**(6): 653–665.
PubMed Abstract | Publisher Full Text | Free Full Text
12. Cárdenas-Navia LI, Mace D, Richardson RA, *et al.*: **The pervasive presence of fluctuating oxygenation in tumors.** *Cancer Res.* 2008; **68**(14): 5812–5819.
PubMed Abstract | Publisher Full Text
13. Dewhirst MW, Secomb TW: **Transport of drugs from blood vessels to tumour tissue.** *Nat Rev Cancer.* 2017; **17**(12): 738–750.
PubMed Abstract | Publisher Full Text
14. Crabtree HG: **Observations on the carbohydrate metabolism of tumours.** *Biochem J.* 1929; **23**(3): 536–545.
PubMed Abstract | Publisher Full Text | Free Full Text
15. van Eunen K, Kiewiet JA, Westerhoff HV, *et al.*: ***Testing biochemistry* revisited: how *in vivo* metabolism can be understood from *in vitro* enzyme kinetics.** *PLoS Comput Biol.* 2012; **8**(4): e1002483.
PubMed Abstract | Publisher Full Text | Free Full Text
16. Coe EL, Greenhouse WV: **Possible regulatory interactions between compartmentalized glycolytic systems during initiation of glycolysis in ascites tumor cells.** *Biochim Biophys Acta.* 1973; **329**(2): 171–182.
PubMed Abstract | Publisher Full Text
17. Chandra FA, Buzi G, Doyle JC: **Glycolytic oscillations and limits on robust efficiency.** *Science.* 2011; **333**(6039): 187–192.
PubMed Abstract | Publisher Full Text
18. van Heerden JH, Wortel MT, Bruggeman FJ, *et al.*: **Lost in transition: start-up of glycolysis yields subpopulations of nongrowing cells.** *Science.* 2014; **343**(6174): 1245114.
PubMed Abstract | Publisher Full Text
19. Hettling H, van Beek JH: **Analyzing the functional properties of the creatine kinase system with multiscale 'sloppy' modeling.** *PLoS Comput Biol.* 2011; **7**(8): e1002130.
PubMed Abstract | Publisher Full Text | Free Full Text
20. Mulquiney PJ, Kuchel PW: **Model of 2,3-bisphosphoglycerate metabolism in the human erythrocyte based on detailed enzyme kinetic equations: equations and parameter refinement.** *Biochem J.* 1999; **342 Pt 3**: 581–596.
PubMed Abstract | Publisher Full Text | Free Full Text
21. Marín-Hernández A, Gallardo-Pérez JC, Rodríguez-Enríquez S, *et al.*: **Modeling cancer glycolysis.** *Biochim Biophys Acta.* 2011; **1807**(6): 755–767.
PubMed Abstract | Publisher Full Text
22. Marín-Hernández A, Rodríguez-Enríquez S, Vital-González PA, *et al.*: **Determining and understanding the control of glycolysis in fast-growth tumor cells. Flux control by an over-expressed but strongly product-inhibited hexokinase.** *FEBS J.* 2006; **273**(9): 1975–1988.
PubMed Abstract | Publisher Full Text
23. Gumaa KA, McLean P: **Sequential control of hexokinase in ascites cells.** *Biochem Biophys Res Commun.* 1969; **35**(6): 824–831.
PubMed Abstract | Publisher Full Text
24. Gumaa KA, McLean P: **A possible interrelationship between binding of hexokinase and the site of ATP formation in Krebs ascites cells.** *Biochem Biophys Res Commun.* 1969; **36**(5): 771–779.
PubMed Abstract | Publisher Full Text
25. Kosow DP, Rose IA: **Origin of the delayed feedback control of glucose utilization in ascites tumor cells.** *Biochem Biophys Res Commun.* 1972; **48**(2): 376–383.
PubMed Abstract | Publisher Full Text
26. Rose IA, Warms JV: **Mitochondrial hexokinase. Release, rebinding, and location.** *J Biol Chem.* 1967; **242**(7): 1635–1645.
PubMed Abstract
27. Glaser G, Giloh H, Kasir J, *et al.*: **On the mechanism of the glucose-induced ATP catabolism in ascites tumour cells and its reversal by pyruvate.** *Biochem J.* 1980; **192**(3): 793–800.
PubMed Abstract | Publisher Full Text | Free Full Text
28. Lambeth MJ, Kushmerick MJ: **A computational model for glycogenolysis in skeletal muscle.** *Ann Biomed Eng.* 2002; **30**(6): 808–827.
PubMed Abstract | Publisher Full Text
29. Chance B, Hess B: **Metabolic control mechanisms. III. Kinetics of oxygen utilization in ascites tumor cells.** *J Biol Chem.* 1959; **234**: 2416–2420.
PubMed Abstract
30. Hess B, Chance B: **Metabolic control mechanisms. VI. Chemical events after glucose addition to ascites tumor cells.** *J Biol Chem.* 1961; **236**: 239–246.
PubMed Abstract
31. Coe EL: **Correlation of glycolytic and respiratory events after addition of a small amount of glucose to Ehrlich ascites carcinoma.** *Cancer Res.* 1966; **26**: 269–275.
Reference Source
32. Coe EL, Ibsen KH, Dixon M, *et al.*: **Glycolysis of small amounts of glucose by Ehrlich ascites carcinoma cells.** *Cancer Res.* 1966; **26**(2): 276–281.
PubMed Abstract
33. Hess B, Chance B: **Phosphorylation efficiency of the intact cell. I. Glucose-oxygen titrations in ascites tumor cells.** *J Biol chem.* 1959; **234**: 3031–3035.
PubMed Abstract
34. Coe EL: **Correlations between adenine nucleotide levels and the velocities of rate-determining steps in the glycolysis and respiration of intact Ehrlich ascites carcinoma cells.** *Biochim Biophys Act.* 1966; **118**(3): 495–511.
PubMed Abstract | Publisher Full Text
35. Coe EL: **Transient isolation of the hexokinase reaction from the glycolytic sequence on initiation of glycolysis in ascites tumor cells.** *Biochem Biophys Res Commun.* 1970; **38**(6): 1105–1112.
PubMed Abstract | Publisher Full Text
36. Lee IY, Coe EL: **Theoretical phosphorylation rates after addition of a small amount of glucose to intact ascites tumor cells.** *Biochim Biophys Acta.* 1967; **131**(3): 441–452.
PubMed Abstract | Publisher Full Text
37. Wu R, Racker E: **Regulatory mechanisms in carbohydrate metabolism. III.**

Limiting factors in glycolysis of ascites tumor cells. *J Biol Chem.* 1959; **234**(5): 1029–1035.
PubMed Abstract

38. Wu R, Racker E: **Regulatory mechanisms in carbohydrate metabolism. IV. Pasteur effect and Crabtree effect in ascites tumor cells.** *J Biol Chem.* 1959; **234**(5): 1036–1041.
PubMed Abstract

39. Lonberg-Holm KK: **A direct study of intracellular glycolysis in Ehrlich's ascites tumor.** *Biochim Biophys Acta.* 1959; **35**: 464–472.
PubMed Abstract | Publisher Full Text

40. Wilhelm G, Schulz J, Hofmann E: **pH-dependence of aerobic glycolysis in ehrlich ascites tumour cells.** *FEBS Lett.* 1971; **17**(1): 158–162.
PubMed Abstract | Publisher Full Text

41. Wilhelm G, Schulz J, Hoffmann E: **[pH-dependence of glycolysis and respiration in Ehrlich ascites tumor cells].** *Acta Biol Med Ger.* 1972; **29**(1): 1–16.
PubMed Abstract

42. van Beek JHGM: **Dataset 1 in: The Dynamic Side of the Warburg Effect: Glycolytic Intermediates as Buffer for Fluctuating Glucose and O_2 Supply in Tumor Cells.** *F1000Research.* 2018.
http://www.doi.org/10.5256/f1000research.15635.d212544

43. Overgaard-Hansen K: **Metabolic regulation of the adenine nucleotide pool. I. Studies on the transient exhaustion of the adenine nucleotides by glucose in Ehrlich ascites tumor cells.** *Biochim Biophys Acta.* 1965; **104**(2): 330–347.
PubMed Abstract | Publisher Full Text

44. van Beek JHGM: **Dataset 2 in: The Dynamic Side of the Warburg Effect: Glycolytic Intermediates as Buffer for Fluctuating Glucose and O_2 Supply in Tumor Cells.** *F1000Research.* 2018.
http://www.doi.org/10.5256/f1000research.15635.d212545

45. Saha J, Coe EL: **Evidence indicating the existence of two modes of glucose uptake in Ehrlich ascites tumor cells.** *Biochem Biophys Res Commun.* 1967; **26**(4): 441–446.
PubMed Abstract | Publisher Full Text

46. van Beek JHGM: **Dataset 3 in: The Dynamic Side of the Warburg Effect: Glycolytic Intermediates as Buffer for Fluctuating Glucose and O_2 Supply in Tumor Cells.** *F1000Research.* 2018.
http://www.doi.org/10.5256/f1000research.15635.d212546

47. Vaupel P, Manz R, Müller-Klieser W, *et al.*: **Intracapillary HbO_2 saturation in malignant tumors during normoxia and hyperoxia.** *Microvasc Res.* 1979; **17**(2): 181–191.
PubMed Abstract | Publisher Full Text

48. Horsman MR, Vaupel P: **Pathophysiological Basis for the Formation of the Tumor Microenvironment.** *Front Oncol.* 2016; **6**: 66.
PubMed Abstract | Publisher Full Text | Free Full Text

49. Dewhirst MW, Kimura H, Rehmus SW, *et al.*: **Microvascular studies on the origins of perfusion-limited hypoxia.** *Br J Cancer Suppl.* 1996; **74**: S247–S251.
PubMed Abstract | Free Full Text

50. Fisher DT, Muhitch JB, Kim M, *et al.*: **Intraoperative intravital microscopy permits the study of human tumour vessels.** *Nat Commun.* 2016; **7**: 10684.
PubMed Abstract | Publisher Full Text | Free Full Text

51. Pigott KH, Hill SA, Chaplin DJ, *et al.*: **Microregional fluctuations in perfusion within human tumours detected using laser Doppler flowmetry.** *Radiother Oncol.* 1996; **40**(1): 45–50.
PubMed Abstract | Publisher Full Text

52. Martinez-Outschoorn UE, Peiris-Pagés M, Pestell RG, *et al.*: **Cancer metabolism: a therapeutic perspective.** *Nat Rev Clin Oncol.* 2017; **14**(1): 11–31.
PubMed Abstract | Publisher Full Text

53. Gullino PM, Grantham FH, Courtney AH: **Glucose consumption by transplanted tumors *in vivo*.** *Cancer Res.* 1967; **27**(6): 1031–1040.
PubMed Abstract

54. Soboll S, Oh MH, Brown GC: **Control of oxidative phosphorylation, gluconeogenesis, ureagenesis and ATP turnover in isolated perfused rat liver analyzed by top-down metabolic control analysis.** *Eur J Biochem.* 1998; **254**(1): 194–201.
PubMed Abstract | Publisher Full Text

55. Buttgereit F, Brand MD: **A hierarchy of ATP-consuming processes in mammalian cells.** *Biochem J.* 1995; **312**(Pt 1): 163–167.
PubMed Abstract | Publisher Full Text | Free Full Text

56. Ainscow EK, Brand MD: **Top-down control analysis of ATP turnover, glycolysis and oxidative phosphorylation in rat hepatocytes.** *Eur J Biochem.* 1999; **263**(3): 671–685.
PubMed Abstract | Publisher Full Text

57. Wieser W, Krumschnabel G: **Hierarchies of ATP-consuming processes: direct compared with indirect measurements, and comparative aspects.** *Biochem J.* 2001; **355**(Pt 2): 389–395.
PubMed Abstract | Publisher Full Text | Free Full Text

58. Vaupel P, Günther H, Grote J, *et al.*: **[Respiratory gas exchange and glucose metabolism of tumors (DS-carcinosarcoma) *in vivo*. I. Experimental investigations of the parameters determining the supply conditions].** *Z Gesamte Exp Med.* 1971; **156**(4): 283–294.
PubMed Abstract | Publisher Full Text

59. van Beek JHGM: **Dataset 4 in: The Dynamic Side of the Warburg Effect: Glycolytic Intermediates as Buffer for Fluctuating Glucose and O_2 Supply in Tumor Cells.** *F1000Research.* 2018.
http://www.doi.org/10.5256/f1000research.15635.d212547

60. Gutenkunst RN, Waterfall JJ, Casey FP, *et al.*: **Universally sloppy parameter sensitivities in systems biology models.** *PLoS Comput Biol.* 2007; **3**(10): 1871–1878.
PubMed Abstract | Publisher Full Text | Free Full Text

61. van Beek JHGM: **Dataset 5 in: The Dynamic Side of the Warburg Effect: Glycolytic Intermediates as Buffer for Fluctuating Glucose and O_2 Supply in Tumor Cells.** *F1000Research.* 2018.
http://www.doi.org/10.5256/f1000research.15635.d212548

62. Kemp A, Mendel B: **How does the Ehrlich ascites tumour obtain its energy for growth?** *Nature.* 1957; **180**(4577): 131–132.
PubMed Abstract | Publisher Full Text

63. Burgess EA, Sylvén B: **Changes in glucose and lactate content of ascites fluid and blood plasma during growth and decay of the ELD ascites tumour.** *Br J Cancer.* 1962; **16**: 298–305.
PubMed Abstract | Publisher Full Text | Free Full Text

64. Klein G: **[Some recent studies on the production and growth characteristics of ascites tumors; a review].** *Z Krebsforsch.* 1956; **61**(2): 99–119.
PubMed Abstract | Publisher Full Text

65. van Beek JHGM: **Dataset 6 in: The Dynamic Side of the Warburg Effect: Glycolytic Intermediates as Buffer for Fluctuating Glucose and O_2 Supply in Tumor Cells.** *F1000Research.* 2018.
http://www.doi.org/10.5256/f1000research.15635.d212549

66. van Beek JHGM: **Dataset 7 in: The Dynamic Side of the Warburg Effect: Glycolytic Intermediates as Buffer for Fluctuating Glucose and O_2 Supply in Tumor Cells.** *F1000Research.* 2018.
http://www.doi.org/10.5256/f1000research.15635.d212550

67. Kroll K, Kinzie DJ, Gustafson LA: **Open-system kinetics of myocardial phosphoenergetics during coronary underperfusion.** *Am J Physiol.* 1997; **272**(6 Pt 2): H2563–H2576.
PubMed Abstract | Publisher Full Text

68. Gray SR, De Vito G, Nimmo MA, *et al.*: **Skeletal muscle ATP turnover and muscle fiber conduction velocity are elevated at higher muscle temperatures during maximal power output development in humans.** *Am J Physiol Regul Integr Comp Physiol.* 2006; **290**(2): R376–382.
PubMed Abstract | Publisher Full Text

69. jhb: **jhvanbeek/Metabolic-model-DSWE: First release. (Version v1.0.0).** *F1000 Research. Zenodo.* 2018.
http://www.doi.org/10.5281/zenodo.1322391

Open Peer Review

Current Referee Status: ✔ ?

Version 1

Referee Report 14 September 2018

doi:10.5256/f1000research.17060.r37981

? **Ziwei Dai**
Duke University School of Medicine, Durham, NC, USA

The manuscript 'The dynamic side of the Warburg effect: glycolytic intermediates as buffer for fluctuating glucose and O2 supply in tumor cells' presents a coarse-grained kinetic model of glycolysis. The model, despite being extremely simplified, is able to reproduce several experimental datasets in Ehrlich ascites tumor cells after parameter calibration. The author then applies this model to predict dynamic behaviors of tumor cells under fluctuating blood flow. I like the idea of using simplified models to interpret complex biological phenomena but would like to see more discussions about the rationale of using this model instead of other models with full details of every reaction involved in glycolysis. There is space to improve presentation of the results as well. Specific comments are listed below for the author's reference.

1. Some important interactions that may affect FBP dynamics are missing in the model. For instance, it is known that FBP is an allosteric activator of pyruvate kinase (Jurica et al[1]; Christofk et al[2]). I expect that this feedback will attenuate the FBP buffering mechanism proposed in this study since lower glycolysis (i.e. 'tail' in this model) is activated by high concentration of FBP thus enhancing its consumption. Moreover, the two sections ('head' and 'tail') of glycolysis are both considered to be irreversible, thus neglecting the effects of thermodynamics on glycolytic flux. This may also lead to overestimation of FBP concentration as well because FBP is not allowed to be converted back to glucose.
2. The main goal of developing this coarse-grained model is not clear to me. Besides the model developed by Chance and Hess, there are numerous mathematical models for glycolysis, most are much more detailed than the model presented in this study. The author claims that this model replaces the model of Chance and Hess – I feel this inappropriate since this statement doesn't give any credit to all other glycolysis models.
3. Most, if not all, results are presented as curves from the simulation with little information about the take-home messages. It is thus very difficult to read the key findings directly from the figures. For instance, it is my understanding that one of the two most important hypotheses drawn based on the simulation is that cells with high glycolytic capacity (which mimics 'Warburgian' cancer cells) consume glucose much more quickly than cells with lower glycolytic capacity after switching from low glucose to high glucose condition, thus being more competitive under conditions with frequent nutrient deprivation. To emphasize this point, I would recommend using one figure directly comparing glucose uptake fluxes in cells with different glycolytic capacities instead of the 10 figure panels currently included in Fig 4.

References

1. Jurica MS, Mesecar A, Heath PJ, Shi W, Nowak T, Stoddard BL: The allosteric regulation of pyruvate

kinase by fructose-1,6-bisphosphate.*Structure*. 1998; **6** (2): 195-210 PubMed Abstract
2. Christofk HR, Vander Heiden MG, Wu N, Asara JM, Cantley LC: Pyruvate kinase M2 is a phosphotyrosine-binding protein.*Nature*. 2008; **452** (7184): 181-6 PubMed Abstract | Publisher Full Text

Is the work clearly and accurately presented and does it cite the current literature?
Partly

Is the study design appropriate and is the work technically sound?
Yes

Are sufficient details of methods and analysis provided to allow replication by others?
Yes

If applicable, is the statistical analysis and its interpretation appropriate?
Yes

Are all the source data underlying the results available to ensure full reproducibility?
Yes

Are the conclusions drawn adequately supported by the results?
Yes

Competing Interests: No competing interests were disclosed.

Referee Expertise: metabolism, epigenetics, computational biology, bioinformatics

I have read this submission. I believe that I have an appropriate level of expertise to confirm that it is of an acceptable scientific standard, however I have significant reservations, as outlined above.

Referee Report 11 September 2018

doi:10.5256/f1000research.17060.r36758

Ranjan K. Dash
Department of Biomedical Engineering, Medical College of Wisconsin and Marquette University, Milwaukee, WI, 53226, USA

This is an interesting original research article based on computational modeling to understand several questions related to cancer cell metabolism, specifically on the Warburg effects and related phenomena (high glucose uptake and lactate production by cancer cells despite sufficient oxygen supply; also very high transient glucose uptake one order of magnitude faster than the high steady state glucose uptake). In doing this, the author developed a new computational model integrating simplified "phenomenological" models of key lumped reactions in glycolysis, mitochondrial ATP synthesis coupled to oxygen consumption (oxidative phosphorylation; OxPhos), and cytosolic ATP consumption. I am not an expert in cancer cell metabolism, so I do not know how much experimental data are available for testing and calibrating the mathematical model. I trust the author has carefully considered all the important experimental data that are available for the calibration of the model. For example, I see the author has

considered some key experimental data sets showing transients in several important variables in the mathematical model governing cellular metabolism in cancer cells (Figure 2). This is surely an important data sets for model calibration, as it depicts the transients of fructose biphosphate (FBP) content, ATP content, glucose uptake, lactate production, and oxygen consumption for two different glucose stimulation conditions in cancer cells (low glucose and high glucose conditions). These data show distinct characteristics in these important variables for these two perturbation conditions. Based on the calibrated model, the author used model simulations to gather several interesting insights into the cancer cell metabolism. Finally, the author has very well recognized the limitations of the model. I still wanted to point out few further limitations of the modeling.

As I mentioned above, the modeling of the lumped reaction processes in this integrated model are highly phenomenological. The author considered two lumped reactions of the whole glycolysis process (termed as "head" and "tail" portion of the glycolysis), one reaction representing OxPhos, and one reaction for ATP consumption. I wonder what is the philosophy behind the formulated flux expressions for these lumped reactions. I see the author has not given any thermodynamic consideration in the modeling of these lumped reactions (e.g. reversible reaction fluxes satisfying the Haldane constraint, relating kinetic parameters to the Gibbs free energy of the lumped reactions). The author has also not included the stoichiometry of the biochemical species in the modeled reaction fluxes. For example, the modeled lumped reaction fluxes do not include square terms considering two ATP and ADP are involved in the lumped phosphorylation-dephosphorylation reactions. Also I am wondering if the author has individually parameterized these reactions fluxes prior to integration and testing the integrated model with the dynamic data in Figure 2.

Besides these few modeling limitations, the author has done a great job in developing, calibrating and testing the model, and coming up with interesting conclusions regarding the operation of this complex metabolic system in cancer cell. I am not sure how these findings can be experimentally tested, but I would invite the author to put some of his thoughts on further testing experimentally these interesting model predictions. Besides, I have few other suggestions:

1. I would suggest the author to show the model simulated reaction fluxes along with the model fittings in Figure 2.

2. I would suggest the author using the acronym EATC throughout after it is defined.

3. I did not see how the effect of blood flow is integrated into the model. I thought the model is for isolated cell experiments in a cuvette.

4. The whole experimental system (cells in buffer) is considered as a single compartment. I am wondering how the model prediction would alter if one considers compartmentation (e.g. extracellular, cytosol, and mitochondria as separate compartments with transport of species in and out of the compartments).

Is the work clearly and accurately presented and does it cite the current literature?
Yes

Is the study design appropriate and is the work technically sound?
Yes

Are sufficient details of methods and analysis provided to allow replication by others?
Yes

If applicable, is the statistical analysis and its interpretation appropriate?
I cannot comment. A qualified statistician is required.

Are all the source data underlying the results available to ensure full reproducibility?
Yes

Are the conclusions drawn adequately supported by the results?
Yes

Competing Interests: No competing interests were disclosed.

I have read this submission. I believe that I have an appropriate level of expertise to confirm that it is of an acceptable scientific standard.